Received: 28 October 2022 | Revised: 15 September 2023 | Accepted: 12 October 2023

DOI: 10.4218/etrij.2022-0391

ORIGINAL ARTICLE

ETRI Journal WILEY

Relay-assisted multiuser MIMO-DQSM system for correlated fading channels

Francisco R. Castillo-Soria[1] | **Carlos Gutierrez**[1] | **Fermin M. Maciel-Barboza**[2] | **Viktor I. Rodriguez Abdala**[3] | **Jayanta Datta**[4]

[1]Telecommunications Department, Faculty of Science, Universidad Autónoma de San Luis Potosí (UASLP), San Luis Potosi, Mexico

[2]Facultad de Ingeniería Mecánica y Eléctrica, Universidad de Colima, Colima, Mexico

[3]Electrical Engineering Academic Unit, Autonomous University of Zacatecas, Zac., Mexico

[4]Department of Electrical Engineering, University of Chile, Santiago, Chile

Correspondence
Francisco R. Castillo-Soria, Telecommunications Department, Faculty of Science, Universidad Autónoma de San Luis Potosí (UASLP), San Luis Potosi, Mexico.
Email: ruben.soria@uaslp.mx

Fermin M. Maciel-Barboza, Facultad de Ingeniería Mecánica y Eléctrica, Universidad de Colima, Colima, Mexico.
Email: fermin_maciel@ucol.mx

Funding information
The authors have no relevant financial interests to declare.

Abstract

This paper presents the performance evaluation of an amplify-and-forward (AF) relay-assisted multiuser multiple input–multiple output (MU–MIMO) downlink transmission system for correlated fading channels. The overall system performance was improved by incorporating a double-quadrature spatial modulation (DQSM) scheme. The bit error rate (BER) performance and detection complexity of the AF–MU–MIMO–DQSM system were analyzed and compared with those of a conventional AF–MU–MIMO system under the same conditions and parameters. The results showed that the correlated fading channel severely affected the performance of systems with higher spectral efficiency (SE). Considering an SE of 12 bpcu/user, the AF–MU–MIMO–DQSM system yielded a gain of up to 3 dB in BER performance compared with that of its conventional counterpart for the analyzed cases. In terms of detection complexity, the AF–MU–MIMO–DQSM system showed a reduction of up to 56 % compared with that of the conventional system for the optimal maximum likelihood detection criterion.

KEYWORDS
AF relay, double–QSM, MIMO systems, multiuser detection

1 | INTRODUCTION

The exponential growth in the number of people and things connected to mobile communication networks and the data traffic generated by them represent a significant challenge for new wireless communication technologies [1, 2]. Existing mobile networks are becoming less capable of meeting the demand, partly due to their inflexible and expensive equipment. Thus, new technologies should be considered. Recently, index modulation (IM) in the spatial domain, which is based on multiple input–multiple output (MIMO) techniques, has been considered for the implementation of sixth-generation networks [3, 4]. In the IM, part of the information is implicitly embedded into the transmitted signal. Therefore, a smaller number of radio frequency chains are

required for MIMO configurations [5]. The word index in the IM refers to any dimension that can be modulated during transmission, including frequency slot, space, transmit (Tx) antenna, code, and channel characteristic types. In particular, spatial modulation (SM) is a novel technique that can be considered part of an IM system. In SM, a complete array of Tx antennas forms a spatial constellation. To transmit input bits, the transmitter activates only one Tx antenna during symbol transmission. If an uncorrelated fading channel is assumed, a different path channel will exist between each Tx and receiver (Rx) antenna. If the receiver knows the channel state information (CSI), it can determine the Tx antenna that has been used to transmit the received symbol [6]. Quadrature SM (QSM) is an improved version of SM. In QSM, the quadrature amplitude modulation (QAM) of the Mth-order (M-QAM) symbol is split into quadrature and in-phase parts to independently represent a spatial symbol [7]. Therefore, QSM increases the SE according to the spatial domain availability by a factor of two transmitted bits. Recently, the concept of QSM has been extended to increase the SE. The extended QSM (EQSM) transmission scheme uses the power dimension to increase the SE of QSM by N times [8]. Hence, an EQSM system using two branches can be considered as double QSM (DQSM) transmission scheme. Therefore, DQSM has double the SE of the QSM scheme.

Specifically, the bits transmitted to each user using the QSM are $m_{\mathrm{QSM}} = \log_2(M) + 2\log_2(L)$ bits per channel use (bpcu) [7], where L is the length of the transmission vector, that is, the number of Tx antennas reserved for a single user. For DQSM, $m_{\mathrm{DQSM}} = 2(\log_2(M) + 2\log_2(L))$ bpcu [8]. A reference scheme using M-QAM modulation and spatial multiplexing (SMux) transmits an $m_{\mathrm{SMux}} = N_t \log_2(M)$ bpcu. For example, for SE = 8 bpcu, DQSM can use 4QAM and $L = 2$ (two Tx antennas per user), whereas the conventional SMux scheme requires 16QAM and two Tx antennas. To ensure a fair comparison, we considered the same SE and number of Tx antennas for both systems under analysis.

On the contrary, relay networks can be used to extend the coverage area [9–12]. In particular, Shang and others [11] investigated secure communications in a cooperative network that included hybrid relay (HR) wireless power, in which an intruder attempts to capture the data transmitted between a user and the HR. In Singh and others [13], the performance of a relay-assisted wireless network over fluctuating fading channels was evaluated. However, a possible drawback of relay-assisted MIMO systems is the complexity of detection, which is caused by the number of antennas used, such as in future massive MIMO (mMIMO) systems [14]. In these systems, the SM and QSM schemes are capable of reducing the complexity of the detectors [15, 16]. For example, in Althunibat and Mesleh [16], two source nodes simultaneously transmitted QSM signals in the same time slot to a relay node. In earlier research [15, 17], QSM techniques were deployed using traditional cooperative communication schemes. More specifically, Castillo-Soria [18] proposed an EQSM-based amplify-and-forward (AF) relay-assisted MU–MIMO downlink transmission system (AF–MU–MIMO), which also uses DQSM. This scheme has better bit error rate (BER) performance than the conventional AF–MU–MIMO–SMux transmission scheme using M-QAM or phase-shift keying (PSK). However, there are presently no reports on the performance of AF–MU–MIMO–DQSM systems over correlated fading channels in terms of the BER and complexity at the receiver. Therefore, in this study, we investigate the BER performance and detection complexity of an AF–MU–MIMO–DQSM system over correlated fading channels. The contributions of this study are as follows:

- The AF–MU–MIMO–DQSM system is evaluated for correlated fading channels. This approach is relevant mainly considering the number of antennas that can be utilized in future mMIMO systems where the effect of spatial correlation is critical to system performance [19].
- The detection complexity of AF–MU–MIMO–DQSM is evaluated and compared with the conventional SMux system for two different configurations and a different number of relays considering the optimal maximum likelihood (ML) detection criterion.

Notably, the complexity of ML detectors is challenging for the implementation of practical systems. Therefore, it is important to develop new detectors with reduced complexities. Various detectors, such as sphere decoding [20, 21], distance-based ordered detection [22], signal vector-based detection [23], and signal vector-based minimum mean square error [24] types, have been proposed to achieve optimal performance at low complexities using SM and QSM systems.

The remainder of this paper is organized as follows. A description of the AF–MU–MIMO–DQSM system model, including DQSM signal generation and its interference cancelation technique, is given in Section 2. Section 3 describes the correlated fading channel model considered, and Section 4 describes the optimal ML detection criterion and evaluates the detection complexity of the systems. The results related to BER performance are then presented in Section 5, and conclusions are summarized in Section 6.

2 | SYSTEM MODEL

Figure 1 shows the AF–MU–MIMO–DQSM system. The system model assumes that there is no direct link between the base station (BS) and the users. Therefore, all communications pass through R relays. The BS has N_t Tx antennas, whereas K users or mobile stations (MSs) that are equipped with N_r receive antennas. The system uses R relays to retransmit received signals using the AF technique. Each relay uses a single Rx/Tx antenna to retransmit the signals received from the BS to K users in the system. Thus, the end-to-end configuration can be considered a $(K \cdot N_r) \times R \times N_t$ relay-assisted downlink MU–MIMO transmission system.

The BS has K DQSM blocks. Each DQSM block is fed with a sequence of input bits, $\boldsymbol{a}_j = \{b_n\}_{n=1}^{m}$, with $b_n \in \{0, 1\}$ intended for the jth user or MS. The output of the jth DQSM block, $\tilde{\mathbf{x}}_j \in \mathbb{C}^{L\times 1}$, is defined as follows:

$$\tilde{\mathbf{x}}_j = [\tilde{x}_1, \tilde{x}_2, ..., \tilde{x}_L]^{\mathrm{T}}, \tag{1}$$

where $\tilde{x}_k \in \{0, s_{\Re}, s_{\Im}\}$ represent the transmitted signal at the kth position. $s_{\Re}$ and $s_{\Im}$ represent the real and imaginary components of the M–QAM symbol, s, respectively. Subsequently, signals $\tilde{\mathbf{x}}_j \in \mathcal{A}$ are precoded and combined to obtain the transmission vector, $\mathbf{x}$, as shown in Figure 1. The transmitted signal, $\mathbf{x}$, at the BS is defined as follows:

$$\mathbf{x} = [x_1, x_2, ..., x_{N_t}]^{\mathrm{T}}. \tag{2}$$

Signal $\mathbf{x}$ is transmitted to R relays through channel matrix $\mathbf{H}^{\mathrm{SR}} \in \mathbb{C}^{R\times N_t}$. The channel between R relays and the jth MS at the destination is defined as $\mathbf{H}_j^{\mathrm{RD}} \in \mathbb{C}^{N_r\times R}$. The uncorrelated fading channel is defined as a Rayleigh wireless channel, where the elements of the matrices, $\mathbf{H}^{\mathrm{SR}}$ and $\mathbf{H}_j^{\mathrm{RD}}$, are independent and identically distributed (i.i.d.) complex Gaussian random variables with a mean of zero and a variance of one, respectively. The correlated fading channel is based on the geometrical model defined in Section 3.

We considered the conventional SMux scheme as the reference system in which all Tx antennas transmit different M-QAM symbols. Therefore, the SE of the SMux is $m_{\mathrm{SMux}} = N_t \log_2(M)$ bpcu.

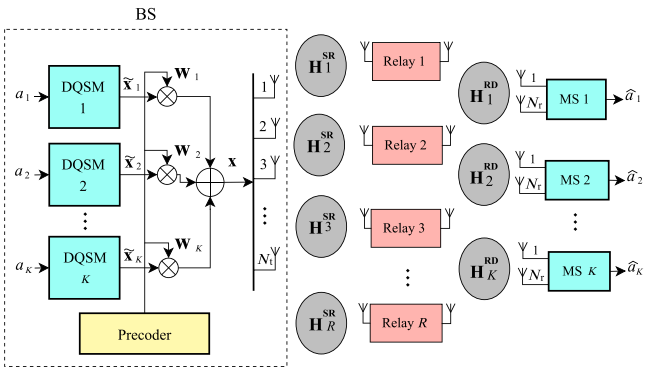

FIGURE 1 Amplify-and-forward (AF) relay-assisted multiuser multiple input–multiple output–double-quadrature spatial modulation (MU–MIMO–DQSM) system model.

2.1 | DQSM signals

Two branches of the previously generated QSM signals are used to generate the DQSM signals because DQSM has good BER performance, low detection complexity, and improved SE compared with the conventional QAM modulation scheme [8]. DQSM signals are generated by adding two QSM signals, $\tilde{x}_1'$ and $\tilde{x}_2'$. Weight factors β_1 and β_2 are used to examine the QSM signals and obtain a normalized output signal.

The signals are then combined to generate the DQSM signal [8] as follows:

$$\tilde{\mathbf{x}}_j = \beta_1 \tilde{x}_1' + \beta_2 \tilde{x}_2'. \tag{3}$$

Figure 2 shows the DQSM transmission block, and Table 1 lists the DQSM mapping rule. Only the first 16 values of the input sequence with $\beta_1 = 1$ and $\beta_2 = 0.5$ were considered in this case. For example, looking the second row of Table 1, the QSM–1 signal is obtained based on the first four input bits. The QSM–2 signal is obtained based on the second four input bits. For the QSM–2 signals, $\mathbf{x}_2'$, the last two bits in column 1 modulate a 4-QAM symbol, $01 \rightarrow (-1+j)$, and the remaining two bits modulate the positions of the real and imaginary parts. That is, the real part of the M-QAM symbol is placed in the first position of the output vector with size $L = 2$. The imaginary part is then assigned to the first

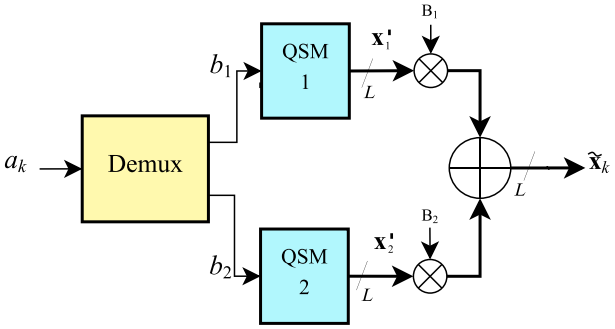

FIGURE 2 Double-quadrature spatial modulation (DQS) transmission block.

TABLE 1 DQSM signals in the transmitter.

Input a_k	QSM-1 x_1'	QSM-2 x_2'	Output DQSM
0000 0000	$1-j$, 0	$1+j$, 0	$1.5-0.5j$, 0
0000 0001	$1-j$, 0	$-1+j$, 0	$0.5-0.5j$, 0
0000 0010	$1-j$, 0	$1-j$, 0	$1.5-1.5j$, 0
0000 0011	$1-j$, 0	$-1-j$, 0	$0.5-1.5j$, 0
0000 0100	$1-j$, 0	1, j	$1.5-j$, $0.5j$
0000 0101	$1-j$, 0	-1, j	$0.5-j$, $0.5j$
0000 0110	$1-j$, 0	1, $-j$	$1.5-j$, $-0.5j$
0000 0111	$1-j$, 0	-1, $-j$	$0.5-j$, $-0.5j$
0000 1000	$1-j$, 0	j, 1	$1-0.5j$, 0.5
0000 1001	$1-j$, 0	j, -1	$1-0.5j$, -0.5
0000 1010	$1-j$, 0	$-j$, 1	$1-1.5j$, 0.5
0000 1011	$1-j$, 0	$-j$, -1	$1-1.5j$, -0.5
0000 1100	$1-j$, 0	0, $1+j$	$1-j$, $0.5+0.5j$
0000 1101	$1-j$, 0	0, $-1+j$	$1-j$, $-0.5+0.5j$
0000 1110	$1-j$, 0	0, $1-j$	$1-j$, $0.5-0.5j$
0000 1111	$1-j$, 0	0, $-1-j$	$1-j$, $-0.5-0.5j$

Abbreviations: DQSM, double-quadrature spatial modulation; QSM, quadrature SM.

position (00 → first position). As $L=2, M=4$, a total of $m_{\text{QSM}}=\log_2(M)+2\log_2(L)=4$ bits can be utilized for each QSM signal in this case. The number of bits that can be transmitted to each MS using the DQSM is $m_{\text{DQSM}}=2(\log_2(M)+2\log_2(L))$ [8]. Therefore, $m_{\text{DQSM}}=8$ bits/user in this example.

2.2 | Interference cancelation

The received signal for the ith relay is [18]

$$y_r^{(i)}=\mathbf{h}_i^{\text{SR}}\mathbf{x}+n_r^{(i)}, \tag{4}$$

where $\mathbf{h}_i^{\text{SR}}$ is the ith row of channel matrix $\mathbf{H}^{\text{SR}}$ and $n_r^{(i)}$ is the noise at the ith relay, which is assumed to be i.i.d. with $\mathcal{CN}(0,\sigma^2)$. The signal received by the relay arrangement can be written in the matrix form as follows:

$$\mathbf{y}_r=\mathbf{H}^{\text{SR}}\mathbf{x}+\mathbf{n}_r, \tag{5}$$

where $\mathbf{n}_r\in\mathbb{C}^{R\times 1}$ denotes a noise vector. These signals are retransmitted by R relays using the AF technique, defined as

$$\mathbf{t}_{\mathbf{x}}=\sqrt{\gamma}\mathbf{y}_r, \tag{6}$$

where γ is the relay amplification factor. The signal received by the jth MS at the destination can then be written as

$$\mathbf{y}_d^{(j)}=\mathbf{H}_j^{\text{RD}}\mathbf{t}_{\mathbf{x}}+\mathbf{n}_d^{(j)}. \tag{7}$$

The received signal, $\mathbf{y}_d^{(j)}\in\mathbb{C}^{N_{\text{r}}\times 1}$, in (7) is a vector containing a combination of all signals transmitted by the relays. By substituting (5) and (6) into (7), we obtain

$$\mathbf{y}_d^{(j)}=\mathbf{H}_j^{\text{RD}}\sqrt{\gamma}\mathbf{y}_r+\mathbf{n}_d^{(j)}=\sqrt{\gamma}\mathbf{H}_j^{\text{RD}}\mathbf{H}^{\text{SR}}\mathbf{x}+\sqrt{\gamma}\mathbf{H}_j^{\text{RD}}\mathbf{n}_r+\mathbf{n}_d^{(j)}. \tag{8}$$

This result can be represented [18] as follows:

$$\mathbf{y}_d^{(j)}=\sqrt{\gamma}\mathbf{H}_j^{\text{Eq}}\mathbf{x}+\mathbf{z}_d^{(j)}, \tag{9}$$

where $\mathbf{H}_j^{\text{Eq}}=\mathbf{H}_j^{\text{RD}}\mathbf{H}^{\text{SR}}\in\mathbb{C}^{N_{\text{r}}\times N_{\text{t}}}$ is defined as the jth equivalent channel matrix and $\mathbf{z}_d^{(j)}=\sqrt{\gamma}\mathbf{H}_j^{\text{RD}}\mathbf{n}_r+\mathbf{n}_d^{(j)}$ is a vector that contains the total noise plus interference component for the jth MS. The complete system can be mathematically described [18] as follows:

$$\begin{bmatrix}\mathbf{y}_d^{(1)}\\ \mathbf{y}_d^{(2)}\\ \vdots\\ \mathbf{y}_d^{(K)}\end{bmatrix}=\sqrt{\gamma}\begin{bmatrix}\mathbf{H}_1^{\text{Eq}}\\ \mathbf{H}_2^{\text{Eq}}\\ \vdots\\ \mathbf{H}_K^{\text{Eq}}\end{bmatrix}\mathbf{x}+\begin{bmatrix}\mathbf{z}_d^{(1)}\\ \mathbf{z}_d^{(2)}\\ \vdots\\ \mathbf{z}_d^{(K)}\end{bmatrix}. \tag{10}$$

The interference generated by multiple users and relays in the system can be eliminated using a precoding matrix, $\mathbf{W}_i\in\mathbb{C}^{N_{\text{t}}\times N_{\text{r}}}$, in the transmission.

$$\mathbf{x}=\sum_{i=1}^{K}\mathbf{W}_i\tilde{\mathbf{x}}_i. \tag{11}$$

By substituting (11) into (9), the received signal, $\mathbf{y}_d\in\mathbb{C}^{N_{\text{r}}\times 1}$, by the jth MS becomes

$$\mathbf{y}_d^{(j)}=\sqrt{\gamma}\mathbf{H}_j^{\text{Eq}}\sum_{i=1}^{K}\mathbf{W}_i\tilde{\mathbf{x}}_i+\mathbf{z}_d^{(j)}, \tag{12}$$

which can be rewritten as follows:

$$\mathbf{y}_d^{(j)}=\sqrt{\gamma}\mathbf{H}_j^{\text{Eq}}\mathbf{W}_j\tilde{\mathbf{x}}_j+\sqrt{\gamma}\mathbf{H}_j^{\text{Eq}}\sum_{i=1,i\neq j}^{K}\mathbf{W}_i\tilde{\mathbf{x}}_i+\mathbf{z}_d^{(j)}, \tag{13}$$

where the first term in (13) is the signal sent to the jth user. The second term is the interference caused by other users in the system, and the third term is noise. The mathematical model of the complete system is represented [18] as follows:

$$\begin{bmatrix} \mathbf{y}_d^{(1)} \\ \mathbf{y}_d^{(2)} \\ \vdots \\ \mathbf{y}_d^{(K)} \end{bmatrix} = \begin{bmatrix} \mathbf{H}_1^{\mathrm{Eq}} & \mathbf{H}_1^{\mathrm{Eq}} & \dots & \mathbf{H}_1^{\mathrm{Eq}} \\ \mathbf{H}_2^{\mathrm{Eq}} & \mathbf{H}_2^{\mathrm{Eq}} & \dots & \mathbf{H}_2^{\mathrm{Eq}} \\ \vdots & & \ddots & \vdots \\ \mathbf{H}_K^{\mathrm{Eq}} & \mathbf{H}_K^{\mathrm{Eq}} & \dots & \mathbf{H}_K^{\mathrm{Eq}} \end{bmatrix} \begin{bmatrix} \mathbf{W}_1\tilde{\mathbf{x}}_1 \\ \mathbf{W}_2\tilde{\mathbf{x}}_2 \\ \vdots \\ \mathbf{W}_K\tilde{\mathbf{x}}_K \end{bmatrix} + \begin{bmatrix} \mathbf{z}_d^{(1)} \\ \mathbf{z}_d^{(2)} \\ \vdots \\ \mathbf{z}_d^{(K)} \end{bmatrix}, \tag{14}$$

where we assume $\sqrt{\gamma} = 1$ for simplicity. Hence, interference can be eliminated if $\mathbf{H}_j^{\mathrm{Eq}}\mathbf{W}_i = \mathbf{0}$, $\forall i \neq j$, where $\mathbf{0}$ is an all-zero matrix. This condition can be written as follows:

$$\overline{\mathbf{H}}_j^{\mathrm{Eq}}\mathbf{W}_j = \mathbf{0},\ j = 1,\ 2,\ \dots,\ K, \tag{15}$$

where $\overline{\mathbf{H}}_j^{\mathrm{Eq}}$ is a matrix containing all system user matrices, apart from that of the jth user. Thus,

$$\overline{\mathbf{H}}_j^{\mathrm{Eq}} = \left[\left(\mathbf{H}_1^{\mathrm{Eq}}\right)^{\mathrm{H}}, \dots, \left(\mathbf{H}_{j-1}^{\mathrm{Eq}}\right)^{\mathrm{H}}, \left(\mathbf{H}_{j+1}^{\mathrm{Eq}}\right)^{\mathrm{H}}, \dots, \left(\mathbf{H}_K^{\mathrm{Eq}}\right)^{\mathrm{H}}\right]^{\mathrm{H}}. \tag{16}$$

Matrix $\mathbf{W}_j$ can be obtained by decomposing matrix $\overline{\mathbf{H}}_j^{\mathrm{Eq}}$ into singular values as follows:

$$\overline{\mathbf{H}}_j^{\mathrm{Eq}} = \mathbf{U}_j\left[\mathbf{\Sigma}_j, \mathbf{0}\right]\left[\mathbf{V}_j^{(1)}\mathbf{V}_j^{(0)}\right]^{\mathrm{H}}, \tag{17}$$

where $\mathbf{U}_j$ is a unitary matrix, $\mathbf{\Sigma}_j$ is a diagonal matrix containing nonnegative singular values of $\overline{\mathbf{H}}_j^{\mathrm{Eq}}$, and $\mathbf{0}$ is an all-zero matrix. Matrix $\mathbf{V}_j^{(1)}$ is composed of vectors corresponding to nonzero singular values, and $\mathbf{V}_j^{(0)}$ is composed of vectors corresponding to zero singular values. Thus, $\mathbf{V}_j^{(0)}$ contains the last N_r columns of $\mathbf{V}_j$, which forms an orthogonal basis in the null space of $\overline{\mathbf{H}}_j^{\mathrm{Eq}}$. Therefore, $\mathbf{V}_j^{(0)}$ can be used as the precoding matrix, $\mathbf{W}_j$. Considering (15), the received signal in (13) is reduced to

$$\mathbf{y}_d^{(j)} = \sqrt{\gamma}\mathbf{H}_j^{\mathrm{Eq}}\mathbf{W}_j\tilde{\mathbf{x}}_j + \mathbf{z}_d^{(j)}, \tag{18}$$

which is an interference-free signal. Finally, considering (15), the complete system is reduced to

$$\begin{bmatrix} \mathbf{y}_d^{(1)} \\ \mathbf{y}_d^{(2)} \\ \vdots \\ \mathbf{y}_d^{(K)} \end{bmatrix} = \begin{bmatrix} \mathbf{H}_1^{\mathrm{Eq}}\mathbf{W}_1 & \dots & \mathbf{0} \\ \mathbf{0} & \dots & \mathbf{0} \\ \vdots & \ddots & \vdots \\ \mathbf{0} & \dots & \mathbf{H}_K^{\mathrm{Eq}}\mathbf{W}_K \end{bmatrix} \begin{bmatrix} \tilde{\mathbf{x}}_1 \\ \tilde{\mathbf{x}}_2 \\ \vdots \\ \tilde{\mathbf{x}}_K \end{bmatrix} + \begin{bmatrix} \mathbf{z}_d^{(1)} \\ \mathbf{z}_d^{(2)} \\ \vdots \\ \mathbf{z}_d^{(K)} \end{bmatrix}. \tag{19}$$

Equation (19) shows the cancelation of the undesired components for all MSs at the destination.

3 | CHANNEL MODEL

The kth channel matrix, $\mathbf{H}_k$, is modeled by assuming that the kth MS is surrounded by a cluster of local interfering objects (IOs) that reflect the transmitted signal, which produces multipath propagation. However, the transmitter is free from IOs. It is further assumed that the BS and K MSs are equipped with uniform linear arrays (ULAs) of antennas. Therefore, following Gutiérrez-Mena and others [25], we characterize $\mathbf{H}_k$ as

$$\mathbf{H}_k = \sum_{\ell=1}^{L'} g_{\ell,k} e^{-j\left(\theta_{\ell,k} + \frac{2\pi}{\lambda}\left[d_{\ell,k}^t + d_{\ell,k}^r\right]\right)} \mathbf{a}_r^{\mathrm{T}}\left(\phi_\ell^r\right)\mathbf{a}_t\left(\phi_\ell^t\right) \tag{20}$$

for $k \in \{1, 2, \dots, K\}$, where L' represents the number of local IOs located near the kth MS. The attenuation factors, $g_{\ell,k}$, are modeled using deterministic quantities given as $g_{\ell,k} = 1/\sqrt{L'}, \forall \ell, k$, whereas the phase shifts, $\theta_{\ell,k}$, are i.i.d. random variables uniformly distributed on the circle. The carrier signal wavelength is denoted by λ, $d_{\ell,k}^t$ denotes the initial distance between the BS and the ℓth IO surrounding the kth MS, and $d_{\ell,k}^r$ denotes the initial distance from the IO to the kth MS. These two distances are determined by the geometrical configuration of the propagation scenario. The distance, $d_{\ell,k}^r$, follows the geometrical one-ring model [25], such that $d_{\ell,k}^r = r_K, \forall k$. Thus, $d_{\ell,k}^t$ is

$$d_{\ell,k}^t = \sqrt{D_k^2 + r_K^2 - 2r\,D\cos\left(\phi_\ell^r\right)}, \tag{21}$$

where D_k is the initial distance between the kth MS and the BS and ϕ_r^k is the angle of arrival (AOA) of the ℓth multipath component (MPC) of $\mathbf{H}_k$. The AOAs are modeled using i.i.d. random variables that are uniformly distributed on the circle. Array vectors $\mathbf{a}_r^T(\phi_\ell^t)$ and $\mathbf{a}_t\left(\phi_\ell^r\right)$ are given by

$$\mathbf{a}_t(\phi_\ell^t) = \left[e^{-jA_1^t \sin(\phi_\ell^t)}, \ \ldots \ , e^{-jA_{N_t}^t \sin(\phi_\ell^t)} \right]^{\mathrm{T}}, \tag{22}$$

$$\mathbf{a}_r(\phi_\ell^r) = \left[e^{-jA_1^r \cos(\phi_\ell^r)}, \ \ldots \ , e^{-jA_{N_r}^r \cos(\phi_\ell^r)} \right]^{\mathrm{T}}. \tag{23}$$

The angle of departure (AOD) of the ℓth MPC of $\mathbf{H}_k$ is denoted as ϕ_ℓ^t. This angle is computed from the corresponding random AOA, ϕ_ℓ^r, as follows:

$$\phi_\ell^t = \arctan\left(\frac{r_K \sin(\phi_\ell^r)}{D_k + r_K \cos(\phi_\ell^r)} \right). \tag{24}$$

Scalar parameters A_t and A_r are

$$A_t = \frac{\pi \Delta_t (1 - N_t)}{\lambda}, A_r = \frac{\pi \Delta_r (1 - N_r)}{\lambda}, \tag{25}$$

where Δ_t and Δ_r denote the distances between the adjacent elements of the ULAs mounted on the BS and MS, respectively.

The spatial cross-correlation of the MIMO channel model defined in this section plays a central role in determining the BER performance of the transmission system. The details of this statistical function are omitted here for brevity; however, the reader can refer to Gutiérrez-Mena and others [25] for a comprehensive description and analysis of the correlation function. Notably, if the number of MPCs is sufficiently large ($L' \geq 7$), then it can be shown that the elements of the kth channel matrix, $\mathbf{H}_k$, are complex-valued standard normal random processes [26]. Therefore, one can state that the envelope of the kth MIMO subchannel follows a first-order Rayleigh distribution [27].

4 | OPTIMAL DETECTION

The detection procedure assumes perfect CSIs at the transmitter and receivers. In this study, the optimal ML detection criterion was used for all systems and configurations. The ML detection criterion for the AF–MU–MIMO–DQSM (hereafter referred to as AF–MU–DQSM) system [18] is defined as

$$\tilde{\mathbf{x}}_j = \mathrm{argmin}_{\tilde{x}} \ _{\mathcal{A}} \| \mathbf{y}_d^{(j)} - \sqrt{\gamma} \mathbf{H}_j^{\mathrm{Eq}} \mathbf{W}_j \tilde{x} \|_{\mathrm{F}}^2. \tag{26}$$

In this study, a perfect CSI was assumed at the transmitter and receiver, which is a common assumption when evaluating system performance. However, the manner in which CSI is transmitted in MIMO systems can pose a challenging task when dealing with relay-assisted systems that also have many antennas at both the transmitter and receiver.

4.1 | Detection complexity

Detection complexity was evaluated by considering the total number of floating-point operations (flops) performed using the ML criterion in (26). Real additions and multiplications require one flop, while 2 and 6 flops are required for complex addition and multiplication, respectively. Division and subtraction require the same number of flops, respectively. Thus, the complex matrix multiplication of $m \times n$ by $n \times p$ requires $8mnp$ flops.

For the reference AF–MU–SMux system, the lattice of the ML detector is defined as

$$\mathbf{G}_j = \mathbf{H}_j^{\mathrm{Eq}} \mathbf{W}_j \mathbf{B}, \tag{27}$$

where matrix $\mathbf{B} \in \mathbb{C}^{N_r \times 2^m}$ is composed of all possible combinations of transmitted symbols. Matrix $\mathbf{H}_j^{\mathrm{Eq}} = \mathbf{H}_j^{\mathrm{RD}} \mathbf{H}^{\mathrm{SR}}$ requires $8N_r R N_t$ flops to be evaluated in a particular receiver. The product, $\mathbf{H}_j^{\mathrm{Eq}} \mathbf{W}_j$, requires $8N_t N_r^2$ flops and generates a matrix with $N_r \times N_r$ dimensions. Furthermore, the multiplication of this matrix by $\mathbf{B}$ requires $8N_r^2 2^m$ flops. Thus, the generation of matrix $\mathbf{G}_j$ requires $8N_r^2(N_t + 2^m)$ flops. Evaluating the differences in (26) requires $2(2^m)N_r$ flops, and evaluating the magnitude utilizes $3N_r 2^m$ flops. Combining these results requires $2(N_r - 1)2^m$ flops, and determining the minimum value in (26) requires $2(2^m)$ flops. Finally, by adding these results, the detection complexity of a general AF–MU–MIMO system is

$$\eta = N_r(8N_t(N_r + R) + 2^m \zeta(8N_r + 7)) \text{ flops}, \tag{28}$$

where ζ is the cardinality of the search space of each topology. For the DQSM system, the cardinality of the constellation is reduced by the zeros inserted in the transmission (when the Tx antenna is turned off). Therefore, for the conventional AF–MU–Smux system, $\zeta = 1$. However, the complexity of the AF–MU–DQSM system can be evaluated by counting the number of zeros inserted into matrix $\mathbf{B}$. The factor, ζ, is evaluated as the number of complex signals used by the DQSM constellation divided by the number of complex signals used by the conventional constellation. In DQSM-based systems, two QSM symbols are transmitted simultaneously, and the same Tx antenna can be used for both. Using an SE of

8 bpcu/user requires a 256-point mesh. The numbers of zeros in the real and imaginary parts of the DQSM constellation are 64. Thus, $\zeta = (256-64)/256 = 0.75$. For the SE of 12 bpcu/user, the value is $\zeta = 0.4375$. Table 2 compares the detection complexity of all configurations in both systems with that of the conventional system. For an SE of 8 bpcu/user, the AF–MU–DQSM system achieved a 22.5% reduction in complexity, whereas for an SE of 12 bpcu/user, it reached up to a 56% reduction from the conventional system.

5 | SIMULATION RESULTS AND DISCUSSION

In this section, we compare the BER performance of the AF–MU–DQSM with that of a conventional AF–MU–SMux system that uses PSK/QAM modulation. For the simulation, the Rayleigh and spatially correlated fading channels described in Section 3 were considered, including the normalized power transmission per user. Table 3 lists the parameters used in the simulations.

Two different configurations were considered to evaluate the performance of the system under the correlated fading channel. First, a $(4\cdot 2)\times R\times 8$ configuration with an SE = 8 bpcu/user was evaluated for 8, 16, and 32 relays in both systems. Note that the AF–MU–DQSM system uses 4-QAM modulation, whereas the conventional AF–MU–SMux scheme requires 16-QAM to achieve the same SE. For the second case, an $(8\cdot 4)\times R\times 32$ configuration with SE = 12 bpcu/user was evaluated for 32, 48, and 64 relays. In this case, the AF–MU–DQSM system used 4-QAM modulation, whereas the conventional AF–MU–SMux scheme requires 8PSK to achieve the same SE.

TABLE 2 Comparison of detection complexities (η).

Spectral efficiency	System configuration	(η), AF–MU SMux	(η), AF–MU DQSM
8 bpcu/user	$(4\cdot 2)\times 8\times 8$	13056 flops	10112 flops
	$(4\cdot 2)\times 16\times 8$	14080 flops	11136 flops
	$(4\cdot 2)\times 32\times 8$	16128 flops	13184 flops
12 bpcu/user	$(8\cdot 4)\times 32\times 32$	675840 flops	316416 flops
	$(8\cdot 4)\times 48\times 32$	692224 flops	332800 flops
	$(8\cdot 4)\times 64\times 32$	708608 flops	349184 flops

Note: All systems were evaluated considering the optimal ML detection criterion, the same SE, and the same number of Rx antennas.
Abbreviations: AF, amplify-and-forward; DQSM, double-quadrature spatial modulation; MU, multiuser.

TABLE 3 Simulation parameters.

Parameter	Value
Power Tx	K
D_k	500 mts.
r_k	50 mts.
L'	20
λ	0.0508 mts.
Speed of MS	50 km/h
Detection	Optimal ML

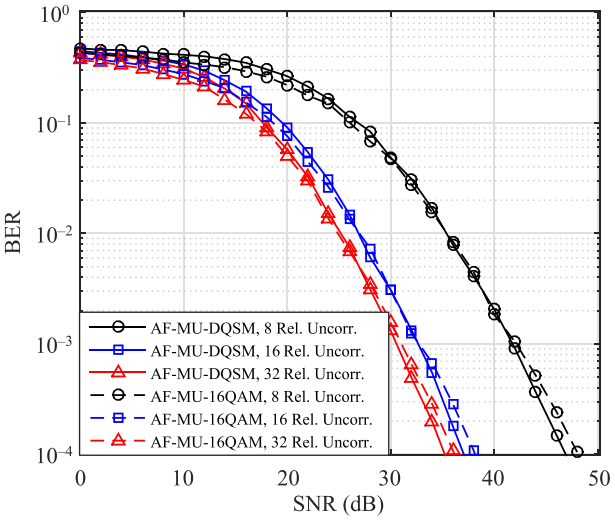

FIGURE 3 Bit error rate (BER) performance comparison of the $(4\cdot 2)\times R\times 8$ configuration (SE = 8 bpcu/user) and the uncorrelated fading channel.

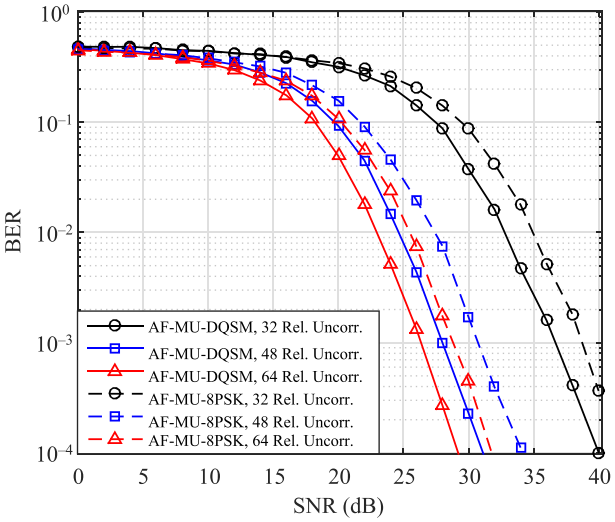

FIGURE 4 Bit error rate (BER) performance comparison of the $(8\cdot 4)\times R\times 32$ configuration (SE = 12 bpcu/user) and the uncorrelated fading channel.

Figures 3 and 4 show that for the $(4 \cdot 2) \times R \times 8$ configuration, a diversity gain of 8–10 dB can be expected when the number of relays in the system increases by 50 %. However, when the number of relays was increased by a similar quantity, the diversity gain increased by only 2 dB.

For the uncorrelated fading channel, the AF–MU–DQSM system performed slightly better than the reference scheme, as shown in Figure 3. Figure 4 shows that for the $(8 \cdot 4) \times R \times 32$ configuration, the AF–MU–DQSM system had 2–3 dB gains compared with the reference scheme. This gain margin was similar for all configurations at different relay quantities.

For the spatially correlated channel, it can be seen that systems with a $(4 \cdot 2) \times R \times 8$ setup had BER performance losses of 2 dB, as shown in Figure 5. However, for the $(8 \cdot 4) \times R \times 32$ setup, both systems were affected by 20 dB–25 dB in BER, as shown in Figure 6. This comparison clearly shows the effect of the correlated channel when the number of Rx/Tx antennas is increased. Spatially correlated channels affected the diversity gain of both systems similarly.

In terms of complexity, the DQSM system clearly outperformed its conventional counterparts. Although both systems suffered from moderate to high complexities derived from singular value decomposition, they operated at the transmitter, where it can be assumed that the BS has sufficient resources to perform the task. The use of optimal ML detectors requires receivers to know the precoding matrices, which can be difficult to ensure. However, the use of optimal ML detectors provided a lower bound for the BER performance of the systems under comparison. The implementation of low-complexity detectors for the AF-MU-MIMO system is an interesting task that will be considered in future studies.

In conclusion, relay-based systems can be used to extend cellular coverage. However, the use of two hops from the transmitter for mobile users increases overall system interference. In addition, MU–MIMO systems increase the system complexity when the number of utilized antennas increases. These results show that the AF–MU–DQSM system outperforms a similar system based on conventional QAM in terms of BER and detection complexity, even in spatially correlated channel scenarios that are characteristic of novel mMIMO communication systems.

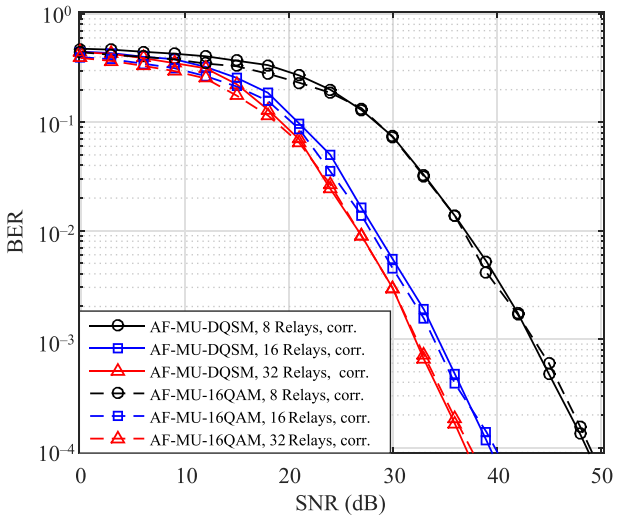

FIGURE 5 Bit error rate (BER) performance comparison for the $(4 \cdot 2) \times R \times 8$ configuration (SE = 8 bpcu/user) and the correlated fading channel.

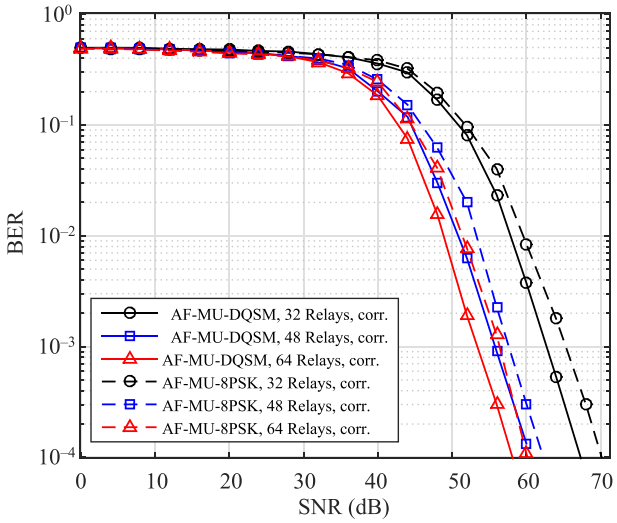

FIGURE 6 Bit error rate (BER) performance comparison for the $(8 \cdot 4) \times R \times 32$ configuration (SE = 12 bpcu/user) and the correlated fading channel.

6 | CONCLUSION

In this study, the BER performance and detection complexity of a relay-assisted AF–MU–DQSM downlink transmission system for correlated fading channels were investigated. The AF–MU–DQSM system was compared with its conventional counterpart under the same conditions and parameters. The results show that the AF–MU–DQSM system has advantages in terms of BER performance and detection complexity compared with the reference scheme. In general, a better BER performance can be expected when an increased number of antennas is utilized. In conclusion, cell coverage can be effectively extended using the AF–MU–DQSM system

with advantages in BER performance and detection complexity. However, the BER performance of systems with higher SE can be severely affected when a correlated fading channel is considered.

CONFLICT OF INTEREST STATEMENT

The authors declare no potential conflicts of interest.

DATA AVAILABILITY STATEMENT

No datasets were generated for this study.

ORCID

Francisco R. Castillo-Soria https://orcid.org/0000-0002-5550-8819
Carlos Gutierrez https://orcid.org/0000-0002-6234-7849
Fermin M. Maciel-Barboza https://orcid.org/0000-0001-5602-355X
Viktor I. Rodriguez Abdala https://orcid.org/0000-0001-7018-4982

REFERENCES

1. P. S. R. Henrique and R. Prasad, *6G the road to the future wireless technologies 2030*, *6G the road to the future wireless technologies 2030*, River Publishers, 2021, pp. i–xxvi.
2. E.-K. Hong, I. Lee, B. Shim, Y.-C. Ko, S.-H. Kim, S. Pack, K. Lee, S. Kim, J.-H. Kim, Y. Shin, Y. Kim, and H. Jung, *6G R&D vision: requirements and candidate technologies*, J. Commun. Netw. **24** (2022), no. 2, 232–245.
3. S. Dang, M. Di Renzo, M. Wen, M. Chafii, Y. Ko, B. F. Uchôa-Filho, and A. Younis, *Editorial: index modulation for 6G communications*, Front. Commun. Netw. **2** (2021), 1–2.
4. R. Dilli, *Design and feasibility verification of 6G wireless communication systems with state of the art technologies*, Int. J. Wirel. Inf. Netw. **29** (2022), 93–117.
5. E. Basar, M. Wen, R. Mesleh, M. Di Renzo, Y. Xiao, and H. Haas, *Index modulation techniques for next-generation wireless networks*, IEEE Access **5** (2017), 16693–16746.
6. H. Bitra and P. Ponnusamy, *Analysis of GSM-SM over $\kappa-\mu$, $\eta-\mu$ and $\alpha-\mu$ fading channels*, Wirel. Pers. Commun. **117** (2021), 2679–2693.
7. R. Mesleh, S. S. Ikki, and H. M. Aggoune, *Quadrature spatial modulation*, IEEE Trans. Veh. Technol. **64** (2014), no. 6, 2738–2742.
8. F. R. Castillo-Soria, J. Cortez, C. A. Gutiérrez, M. Luna-Rivera, and A. Garcia-Barrientos, *Extended quadrature spatial modulation for MIMO wireless communications*, Phys. Commun. **32** (2019), 88–95.
9. N. T. Nguyen, Q.-D. Vu, K. Lee, and M. Juntti, *Hybrid relay-reflecting intelligent surface-assisted wireless communications*, IEEE Trans. Veh. Technol. **71** (2022), no. 6, 6228–6244.
10. N. Qi, W. Wang, D. Ye, M. Wang, T. A. Tsiftsis, and R. Yao, *Energy-efficient full-duplex UAV relaying networks: trajectory design for channel-model-free scenarios*, ETRI J. **43** (2021), no. 3, 436–446.
11. X. Shang, H. Yin, Y. Wang, M. Li, and Y. Wang, *Secure multiuser scheduling for hybrid relay-assisted wireless powered cooperative communication networks with full-duplex destination-based jamming*, IEEE Access **9** (2021), 49774–49787.
12. S. Yunlong and T. A. Gulliver, *Precoding for multiuser MIMO full-duplex amplify-and-forward relay uplink communication systems*, SN Appl. Sci. **2** (2020), no. 4, 1–7.
13. S. Singh, D. Mitra, and R. K. Baghel, *Performance evaluation of relay assisted wireless powered network over fluctuating two ray fading channel with diversity reception*, Wirel. Pers. Commun. **121** (2021), 1739–1755.
14. W. Belaoura, K. Ghanem, M. Z. Shakir, and M. O. Hasna, *Performance and user association optimization for UAV relay-assisted mm-wave massive MIMO systems*, IEEE Access **10** (2022), 49611–49624.
15. A. Afana, R. Mesleh, S. Ikki, and I. E. Atawi, *Performance of quadrature spatial modulation in amplify-and-forward cooperative relaying*, IEEE Commun. Lett. **20** (2015), no. 2, 240–243.
16. S. Althunibat and R. Mesleh, *Performance analysis of quadrature spatial modulation in two-way relaying cooperative networks*, IET Commun. **12** (2018), no. 4, 466–472.
17. A. Afana, E. Erdogan, and S. Ikki, *Quadrature spatial modulation for cooperative MIMO 5G wireless networks*, (IEEE Globecom Workshops (GC Wkshps), Washington, DC, USA), 2016, pp. 1–5.
18. F. R. Castillo-Soria, *AF relay assisted multiuser MIMO-DQSM downlink transmission system*, Electron. Lett. **56** (2020), 682–684.
19. S. Li, P. J. Smith, P. A. Dmochowski, and J. Yin, *Analysis of analog and digital MRC in massive MU-MIMO systems over correlated channels*, J. Commun. Netw. **23** (2021), no. 6, 454–462.
20. F. R. Castillo-Soria, J. Cortez, F. M. R. Maciel-Barbosa, V. I. Rodríguez-Abdalá, and R. Palacio, *Low complexity detection for an AF relay assisted MIMO QSM system*, (IEEE 10th Annual Information Technology, Electronics and Mobile Communication Conference (IEMCON), Vancouver, Canada), 2019, pp. 689–694.
21. A. Younis, S. Sinanovic, M. Di Renzo, R. Mesleh, and H. Haas, *Generalised sphere decoding for spatial modulation*, IEEE Trans. Commun. **61** (2013), no. 7, 2805–2815.
22. Q. Tang, Y. Xiao, P. Yang, Q. Yu, and S. Li, *A new low-complexity near-ML detection algorithm for spatial modulation*, IEEE Wirel. Commun. Lett. **2** (2013), no. 1, 90–93.
23. J. Wang, S. Jia, and J. Song, *Signal vector based detection scheme for spatial modulation*, IEEE Commun. Lett. **16** (2012), no. 1, 19–21.
24. J. Li, X. Jiang, Y. Yan, W. Yu, S. Song, and M. H. Lee, *Low complexity detection for quadrature spatial modulation systems*, Wirel. Pers Commun. **95** (2017), 4171–4183.
25. J. T. Gutiérrez-Mena, C. A. Gutiérrez, M. Luna-Rivera, D. U. Campos-Delgado, and J. Vázquez-Castillo, *A novel geometrical model for non-stationary MIMO vehicle-to-vehicle channels*, IETE Tech. Rev. **36** (2019), no. 1, 27–38.
26. M. Pätzold, *Mobile radio channels*, Second, John Wiley and Sons, Chichester, UK, 2011.
27. C. A. Gutiérrez, J. T. Gutiérrez-Mena, J. M. Luna-Rivera, D. U. Campos-Delgado, R. Velázquez, and M. Pätzold, *Geometry-based statistical modeling of non-WSSUS mobile-to-mobile rayleigh fading channels*, IEEE Trans. Veh. Technol. **67** (2017), no. 1, 362–377.

AUTHOR BIOGRAPHIES

Francisco R. Castillo-Soria received his bachelor and master of Science degrees in Telecommunications Engineering from the National Polytechnic Institute (IPN-ESIME), Mexico City, Mexico, in 2000 and 2004, respectively. He received his Doctor of Science degree in Electronics and Telecommunications from the Ensenada Center of Scientific Research and Higher Education (CICESE), Ensenada B.C., Mexico, in 2015. Since 2017, he has been a full-time professor at the Autonomous University of San Luis Potosi, S.L.P., Mexico. His current research interests include spatial/index modulation and RIS-assisted multiuser MIMO communication systems.

Carlos Gutierrez received his B.E. degree in Electronics and Digital Communication systems from Universidad Autónoma de Aguascalientes, Mexico, in 2002, his Advanced Studies Diploma in signal processing and communication theory from Universidad Politécnica de Cataluña, Spain, in 2005, his M.S. degree in Electronics and Telecommunications from CICESE, Mexico, in 2006, and his Ph.D. degree in Mobile Communication Systems from the University of Agder, Norway, in 2009. From 2009 to 2011, he attended the School of Engineering at Universidad Panamericana, Aguascalientes, Mexico. Since January 2012, he has been with the Faculty of Science, Universidad Autónoma de San Luis Potosí, Mexico. His research interests include the modeling, simulation, and measurement of wireless channels, antenna design, vehicular communications, and wireless perception systems for human activity recognition.

Fermin M. Maciel-Barboza received his bachelor degree in Communications and Electronics and his master of Engineering degree from the University of Colima in 2010 and 2012, respectively. He graduated with a doctor of science degree in Electronics and Telecommunications from the Center for Scientific Research and Higher Education of Ensenada, Baja California, Mexico, in 2016. He works as a research professor in the Faculty of Mechanical and Electrical Engineering at the University of Colima. His areas of interest are multi-user MIMO network management, interference mitigation, and network optimization with cooperative and competitive approaches.

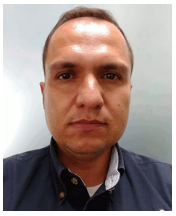

Viktor I. Rodriguez-Abdala received his BS degree in Computational Sciences and Telecommunications Engineering from Technological University in Baja California, La Paz, B.C.S., Mexico, in 2002 and his MS and D.Sc. degrees in Electronics and Telecommunications from the Center for Scientific Research and Higher Education at Ensenada, B.C., in 2005 and 2016, respectively. Since 2018, he has been working at the Autonomous University of Zacatecas, Zacatecas, Mexico, and is currently a research professor with a postgraduate degree in Engineering in Technological Innovation at the Electrical Engineering Academic Unit. His main research interests include digital signal processing for digital communications, software-defined radio, and low-power wide-area networks.

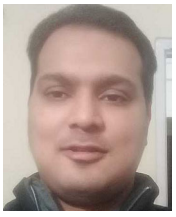

Jayanta Datta received his B-tech degree in Computer Science and Engineering from the Institute of Engineering and Management, Kolkata, India, in 2007. He received the MS and Ph.D. degrees in Electrical Engineering from the Illinois Institute of Technology, Chicago, USA, and the National Taipei University of Technology, Taipei, Taiwan, in 2009 and 2019, respectively. He was associated with the Indian Institute of Technology, Kharagpur (IIT-KGP) from 2019 to 2021, where he worked as a senior research fellow. He has been working at the University of Chile as a postdoctoral research fellow since 2022. His research focuses on signal processing and wireless communications, filter-bank-based multicarrier waveform design, cyclostationary signal processing, adaptive beamforming, compressive sensing, speech enhancement, and deep neural networks.

How to cite this article: F. R. Castillo-Soria, C. Gutierrez, F. M. Maciel-Barboza, V. I. Rodriguez Abdala, and J. Datta, *Relay-assisted multiuser MIMO-DQSM system for correlated fading channels*, ETRI Journal **46** (2024), 184–193. DOI 10.4218/etrij.2022-0391